Flexible diamond-like carbon films on rubber

Pei, Y.T.; Bui, X.L.; Pal, J.P. van der; Martinez-Martinez, D.; Zhou, X.B.; Hosson, J.Th.M. De

Published in:
Acta Materialia

DOI:
10.1016/j.actamat.2012.07.017

Available online at www.sciencedirect.com

SciVerse ScienceDirect

Acta Materialia 60 (2012) 5526–5535

Acta MATERIALIA

www.elsevier.com/locate/actamat

Flexible diamond-like carbon films on rubber: On the origin of self-acting segmentation and film flexibility

Y.T. Pei [a,*], X.L. Bui [a], J.P. van der Pal [a], D. Martinez-Martinez [a], X.B. Zhou [b], J.Th.M. De Hosson [a]

[a] *Materials Innovation Institute M2i, Department of Applied Physics, University of Groningen, Nijenborgh 4, 9747 AG Groningen, The Netherlands*
[b] *SKF Engineering and Research Center, Kelvinbaan 16, 3439 MT Nieuwegein, The Netherlands*

Received 23 March 2012; received in revised form 2 July 2012; accepted 4 July 2012

Abstract

This paper reports an experimental approach to deposit flexible diamond-like carbon (DLC) films on hydrogenated nitrile butadiene rubber (HNBR) with plasma-assisted chemical vapor deposition and an analytical model to describe the self-segmentation mechanism of the DLC films. By making use of the substantial thermal expansion mismatch between the DLC films and the rubber substrate, a dense network of cracks forms in the DLC films and contributes to flexibility. The size of the microsegments can be controlled by tuning the temperature variation of the substrate during deposition through varying the substrate bias voltage. The formation mechanism of the crack network and its effect on the flexibility of DLC films coated on rubber are presented.

Keywords: Diamond-like carbon films; Plasma chemical vapor deposition; Self-segmentation; Flexibility; Adhesion

1. Introduction

Rubber seals are widely used in lubrication systems and bearings to avoid leakage of lubricants and to prevent dirt and water entering the system. With its excellent elasticity, rubber can absorb mechanical impact and seals well in dynamic contact. However, rubbers exhibit very high coefficients of friction (CoF) when sliding against most engineering materials (CoF = 1–6), being the major source of friction in lubrication systems or bearings where dynamic rubber seals are employed. Furthermore, the rubber surface can be easily damaged at high sliding velocity and tends to adhere to the counterpart. Under heavy working conditions, rubber seals are subjected to severe wear leading to an increase in clearance, which is often the cause of loss of function and failure of the lubrication system. Applying a wear-resistant coating with low friction is an advanced solution to enhance the performance of rubber seals [1–3].

For a rigid protective film deposited on compliant substrates such as rubbers, the most critical issues that determine the performance of the entire system are the flexibility of the film and interfacial adhesion. Sufficient flexibility of the protective film is required to adapt large deformations of rubber substrates under loading and can be achieved through film segmentation. Strong adhesion is a prerequisite, ensuring that the segments of the film adhere well to the rubber substrates and maintain functionality under loading condition. In particular, the combination of flexibility and strong adhesion is crucial for diamond-like carbon (DLC) films coated on dynamic rubber seals where cyclic and large elastic deformation may be exerted.

In the past, a tile-like patterned film on rubber was proposed and deposited by using a net mask in front of the substrate [1]. However, there are technical problems with

* Corresponding author.
E-mail addresses: y.pei@rug.nl (Y.T. Pei), j.t.m.de.hosson@rug.nl (J.Th.M. De Hosson).

1359-6454/$36.00
http://dx.doi.org/10.1016/j.actamat.2012.07.017

this approach: the size of the film segments is limited to the sub-millimeter range, and there are open gaps of at least tens of micrometers (equal to the thickness of the grid) between the film segments. Experimental results revealed that the impact between the asperity on the surface of the sliding counterpart and the sharp edges of the open cracks in the films produced a large amount of debris that led to high friction and severe wear of the coated rubber [2].

In this paper, we report another approach for depositing microsegmented DLC films of superior flexibility on rubber. The novelties are that the segmentation process of the DLC films is self-acting and self-adjusting throughout the deposition, and that the size of the film segments separated by the close crack network can be controlled well at much smaller length scales. The mechanism of formation of the crack network during deposition is examined and presented. The interfacial adhesion strength and flexibility of the DLC films are also investigated with in situ scanning electron microscopy (SEM) tensile tests.

2. Experimental procedures

Hydrogenated nitrile butadiene rubber (HNBR) sheet of 2 mm thickness was used as the substrate in this work. The brownish HNBR substrates, 45×45 mm^2 in size, were first cleaned with a solution of detergent (Superdecontamine 33 from N.V. Intersciences S.A., Brussels) in an ultrasonic cleaner and then rinsed with demineralized water. Thereafter, wax removal was carried out in an ultrasonic tank with hot demineralized water (90–95 °C) [3]. This washing process with hot water was repeated three times. Next, the HNBR substrates were dried in a centrifugal machine and then heated up to 120 °C for 15 min in order to evaporate all the absorbed water. The substrates were subsequently cooled to room temperature in ambient air before being loaded into the deposition chamber. The instrumental modulus of the HNBR rubber, as determined by a method described elsewhere [4], is 10.2 MPa and its surface roughness is 0.35 μm, as measured after wax removal using laser confocal microscopy. The HNBR has a typical coefficient of thermal expansion of 1.8×10^{-4} K^{-1}.

Plasma cleaning of the rubber substrates and deposition of DLC films were carried out in a Teer UDP400/4 closed-field unbalanced magnetron sputtering system with all four magnetrons powered off. A pulsed DC power unit (Pinnacle plus, Advanced Energy) was used for substrate bias source, operating at 250 kHz and 87.5% duty cycle. The HNBR substrates were cleaned by Ar plasma for 30, 35, 40 and 45 min at bias voltages of −600, −500, −400 and −300 V, respectively. During the last 10 min of the plasma cleaning, hydrogen gas was added (50%) for reactive plasma cleaning to enhance the interface adhesion of DLC films. Immediately after the plasma cleaning treatment, DLC films were deposited by plasma-assisted CVD (PACVD) at pulsed DC bias voltages of −300, −400 and −500 V for 120, 60 and 45 min, respectively, to reach the same film thickness of 300 ± 20 nm. The films are thus named as DLC*xxx*–*yyy*V or DLC*xxx*–*yyy*/*zzz*V, e.g. DLC600–400 V and DLC300–600/400 V, where *xxx* is the substrate bias voltage (in volts) used in the plasma cleaning and *yyy* (*zzz*) is the bias voltage for the deposition. It is common practice for the electric power (pulsed DC, DC, rf, etc.) applied to bias the substrate and to maintain the plasma in PACVD to be operated in voltage-control mode, so we did this too. The total power is proportional to the coating load (namely the amount or the size/area of the substrates) and is affected by the conductivity of the substrate material. Therefore, the power is not a very indicative parameter for the PACVD process when different loads are used to coat batches and or different coating rigs are used. Rather, the primary parameter of PACVD is the substrate bias voltage that determines the intensity of the plasma. The ratio of gas flow rates was set at $Ar{:}C_2H_2 = 3{:}2$, with a constant process pressure of 3×10^{-3} mbar. However, as the inlet pipeline was also used for acetylene, residual hydrogen might be present for the first 10 min of deposition, during which time the growth of the DLC film was only minor. The HNBR substrates were rotated at a revolving speed of 3 rpm during the deposition. The substrate temperature during the plasma etching/deposition was measured in situ with a thermocouple inserted into the rubber sheet substrate.

The flexibility and adhesion strength of the DLC film were examined via in situ stretch tests on coated specimens of gauge section dimensions $10 \times 3 \times 2$ mm^3, with a home-made tensile stage installed in a Philips XL-30 FEG scanning electron microscope. The surface morphology and microstructure of DLC films on rubber were characterized by means of SEM, with the fracture cross-sections of DLC film-coated rubber samples made after being cooled in liquid nitrogen for 10 min.

3. Results

3.1. Temperature variation of rubber substrates in deposition

The measured temperature evolution of rubber substrates during plasma cleaning and successive deposition is shown in Fig. 1. The temperature variation (ΔT) of HNBR substrates during deposition is related to the bias voltage used for the PACVD process and the substrate temperature at the beginning of deposition. The plasma is considered as the 'hot body' whose temperature (T_{plasma}) is constant and dependent solely on the bias voltage applied. The heat flow from the "hot" plasma to the "cold" substrate, which changes the temperature of the substrate as a result, depends on the temperature difference between the plasma and the substrate. From the Fourier heat conduction equation, the temperature of a rubber substrate under plasma treatment follows

$$T = (T_0 - T_{\text{plasma}}) \times e^{-Kt} + T_{\text{plasma}} \quad (1)$$

where T_0 is the initial temperature of rubber substrate and t represents the time of treatment. The measured substrate

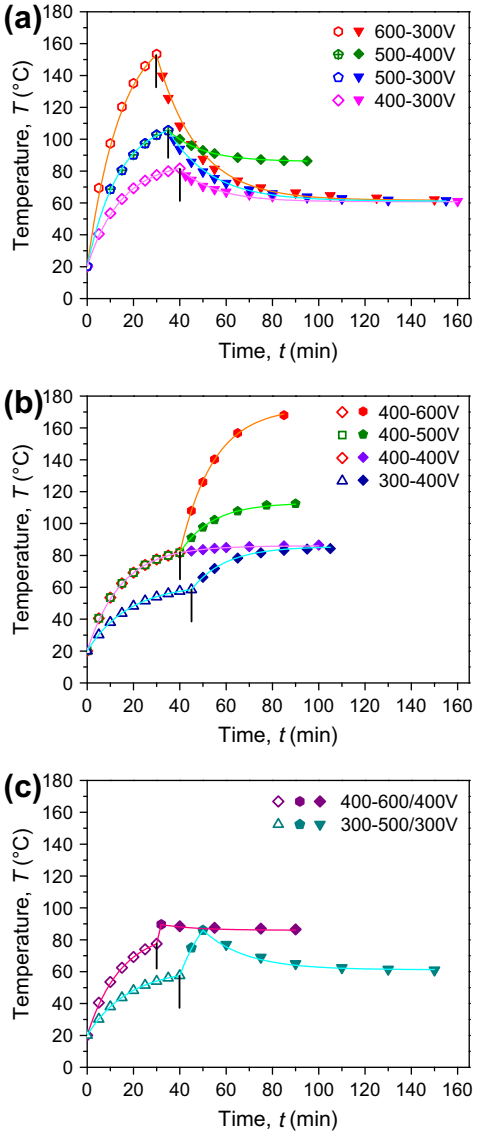

Fig. 1. Evolution of measured substrate temperature vs. time of plasma cleaning (open symbols) and deposition (close symbols), with the solid curves fitted according to Eq. (1): (a) temperature drop (negative ΔT), (b) temperature increase (positive ΔT) and (c) a combination of temperature increase and drop, exposed during deposition with different substrate bias voltages. Vertical bars indicate the transition moment from plasma cleaning to deposition process.

temperatures vs. time of plasma treatment (cleaning and deposition) can be fitted well by Eq. (1), as indicated by the solid curves in Fig. 1. By finding the exponential factor K for different rubbers, various amplitudes of ΔT can be readily designed for the control of segmentation (as to be discussed in the following sections) by changing the bias voltage against deposition time. For instance, negative ΔTs of different amplitudes were obtained by applying a lower substrate bias voltage than the one used for plasma cleaning (Fig. 1a). Vice versa, positive ΔTs of different amplitudes were generated by increasing the substrate bias voltage during deposition (Fig. 1b). Moreover, positive and negative ΔTs can be combined to realize a more complicated temperature profile in a single deposition process (Fig. 1c), which may be used to control the flatness of the DLC film segments, as shown in the next section. It should be pointed out that, technically, external heating and/or cooling can also regulate the temperature profiles of the substrates for the same purpose.

3.2. Self-segmentation of DLC films and segment shape

The surface morphology of DLC thin films on HNBR deposited under varying substrate temperature is characterized by crack networks, as shown in Fig. 2. The effective temperature variation exposed during deposition governs the expansion or shrinkage of the rubber substrates, and thus the mismatch stress in a growing DLC film, which in turn determines the spacing of the crack network or the size of DLC film segments. It is understood that a positive ΔT or tensile stress in the growing DLC film leads to the formation of a crack network once the stress is beyond the strength of the DLC film and that the size of the film segments is related to the amplitude of ΔT (see Fig. 2a and b). In contrast, a negative ΔT or compressive stress results in the formation of wrinkles and, due to bending fracture, also eventually leads to a crack network whose density is likewise governed by the amplitude of ΔT (Fig. 2c and d). Fig. 3 plots the average size of the DLC film segments (or equivalently the average spacing of crack network) vs. the absolute value of the temperature variation ΔT. It is clear that a larger value of ΔT yields smaller segments of DLC film. Moreover, the size of the DLC film segments can changed over a wide range, from hundreds to tens of micrometers, by regulating the ΔT of the rubber substrate during plasma deposition.

The surface morphology of the film segments reflects the different states of deformation: the film segments formed under a tensile misfit stress (positive ΔT) are rather flat (see Fig. 4a), whereas those generated under continuous compression (negative ΔT) are convexly curved, as shown in Fig. 4b. It is noteworthy that, in both cases, the edges of all the segments bend inwards and thus form a crack–groove network. The geometry of such a crack–groove network surrounding the DLC film segments is attributed to the final shrinkage of rubber substrate as it cools down to room temperature after deposition has finished. When the segments adhere strongly to the rubber substrate, they are pushed against each other during the shrinkage of the rubber substrate and bend inwards along the edge where the highest compressive strain occurs. It must be emphasized that the inwardly bent edge of the DLC film segments and the close crack network are crucial for avoiding the impact between the surface asperities of the sliding counterpart and the otherwise sharp edges of open cracks in a film, thus preventing the formation of a large amount of wear debris that can cause wear and high friction in practical applications [2]. In addition, the groove network may also serve as a microreservoir for lubricants for dynamic rubber seals in heavy work conditions. Fig. 4c shows a

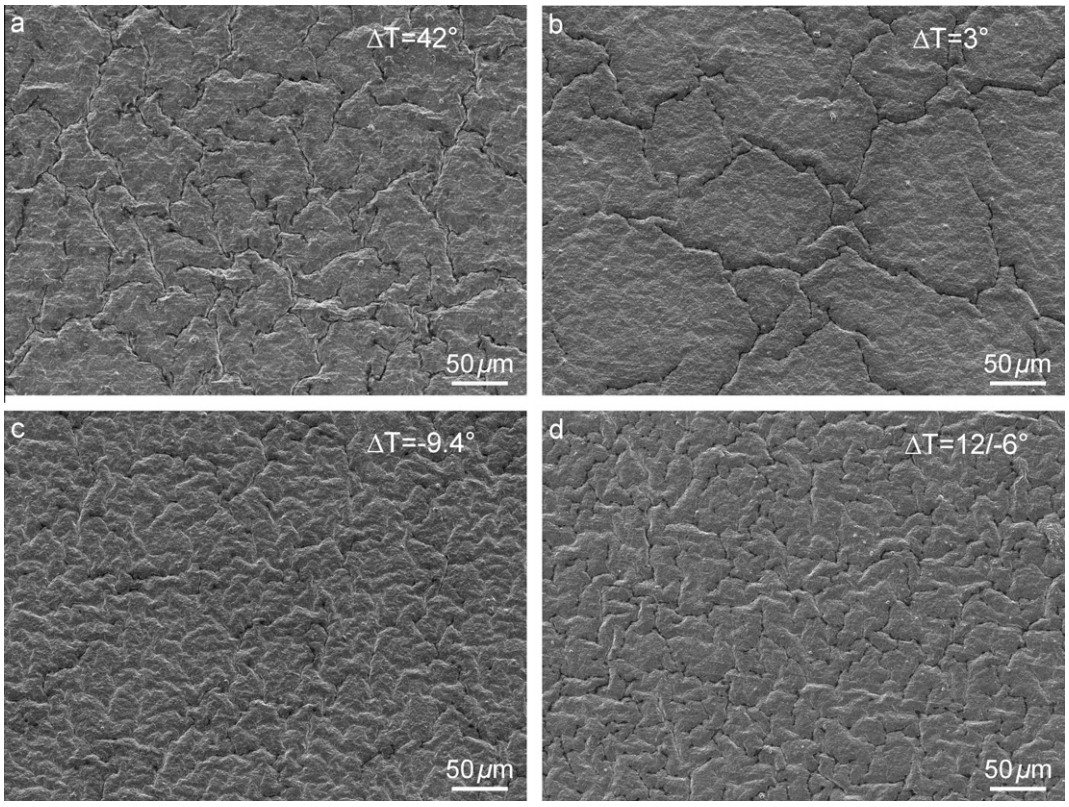

Fig. 2. Surface morphology of DLC films on HNBR deposited with different temperature variations: (a) $\Delta T = 42$ °C (DLC400–600 V), (b) $\Delta T = 3$ °C (DLC400–400 V), (c) $\Delta T = -9.4$ °C (DLC400–300 V) and $\Delta T = 12/-6$ °C (DLC400–600/400 V).

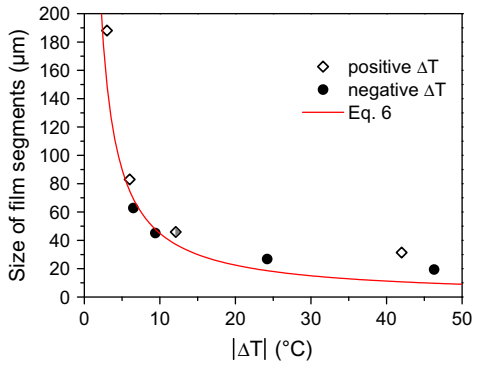

Fig. 3. Size of DLC film segments vs. the absolute value of effective temperature variation of the rubber substrate during deposition.

close-up view of a typical fracture cross-section of a DLC film that exhibits a columnar structure and conforms to the rough surface of the rubber substrate.

3.3. Flexibility and adhesion strength of DLC films

An in situ SEM tensile test was used to examine the flexibility and adhesion strength of the DLC films on HNBR rubber. Fig. 5 presents the evolution of fracture patterns in a DLC400–400 V film with applied tensile strain. Up to 4% tensile strain, no fracture crack was observed to nucleate in the DLC film segments; rather, elongation, rotation and translation of the segments occurred, indicating that the DLC film with a 188 μm segment size exhibits a strain tolerance of ~4% without the formation of fracture cracks. At about 4.5% tensile strain, new longitudinal cracks parallel to the loading direction first occurred in large DLC segments attributed to the crease induced by transverse compression of the rubber substrate. At 5% strain, the first transverse fracture crack appeared, as shown in Fig. 5b, where an overlay of dashed line network indicates the original crack network prior to deformation, revealing the expansion, rotation and translation of the DLC film segments mentioned above. With further increasing tensile strain (Fig. 5c and d), more new fracture cracks (both longitudinal and transverse) formed and the previously formed transverse cracks continuously opened. At 50% tensile strain, the largest opening of transverse cracks reached several micrometers, about half of the average length of the fractured patches, as shown in Figs. 5e and 6a and b. In the open cracks, the underlying rubber substrate was locally pulled out and stretched to form a fiber texture with large elongated voids due to stress localization (see Fig. 6b). It is noteworthy that the longitudinal creases did not lead to the formation of debonding film "bridges", as observed in the DLC film deposited on PET sheet [6], due to the substrate buckling under straining. Instead, the DLC film adhered tightly over the buckled surface of

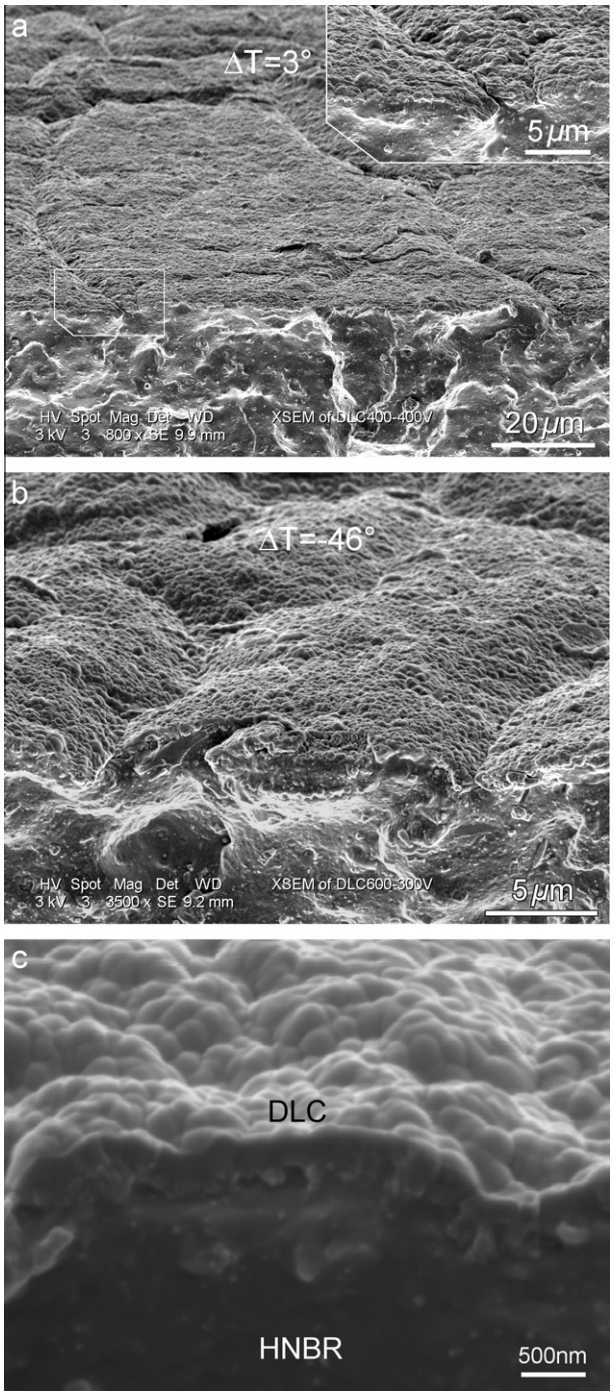

Fig. 4. Fracture cross-section of DLC film-coated HNBR showing the profile of the DLC film segments: (a) flat segments of DLC400–400 V formed under tensile stress ($\Delta T = 3$ °C) and (b) convexly curved segments of DLC600–300 V deposited under compressive stress ($\Delta T = -46$ °C). In both the cases, the edges of the segments bend inwards. (c) A close-up view of typical fracture cross-section of the DLC films.

HNBR rubber and was creased to form close cracks with the edges bent inwards, driven by the transverse compression of rubber substrate, as shown in Fig. 6b and the inset. After unloading, the DLC film segments touched each other and all the cracks closed again: see Figs. 5f and 6c, where the transverse and longitudinal fracture cracks, in brighter contrast, intersect each other in comparison with the irregular growth crack network, in dark contrast. The most important message of the tensile tests is that the fractured DLC film patches or segments do not debond even under such a large deformation, indicating superb interface adhesion and flexibility.

The strain tolerance of DLC films is mainly related to the average size of the DLC film segments and the compression strain built up during the cooling phase of coated rubber substrates after deposition. The DLC films with finer segments exhibit greater strain tolerance, about 7% in the case of DLC400–300 V film with an average segment size of 45 μm. It is understandable that a denser growth crack network in the DLC film may accommodate a larger applied strain (before the formation of fracture cracks) in several ways: flattening of the curved film segments, and especially the bent segment edges, to release the residual compression strain built up in deposition, and the elongation of DLC film segments via the loosening of column boundaries and the opening of a dense growth microcrack network. As the strain increased beyond the strain tolerance (e.g. 8% in Fig. 7b), transverse fracture cracks occurred in the DLC film segments. With further increasing strain, more transverse fracture cracks formed and continuously opened (Fig. 7c and d). However, longitudinal cracks rarely formed below 50% strain (Fig. 7e). The reason for this was that the much finer film segments and the denser growth cracks facilitate transverse buckling of the rubber substrate. To adapt the large transverse compression of the rubber substrate, the fine film segments just needed to curve further along the transverse direction. Apart from the transverse fracture cracks, the surface morphology of the stretched DLC film of fine segments shows little change from the original one after unloading from 50% tensile strain (see Fig. 7f and a), indicating ever better flexibility than that of DLC films of larger segments. In particular, there was no debonding of the fractured film patches.

Upon tensile straining, a shear stress $\tau(x)$ is developed at the interface of DLC film and the rubber substrate, and causes a tensile stress $\sigma(x)$ in the film segments, x being the distance from the segment edge. When the strain is sufficient, the tensile stress reaches the ultimate tensile strength σ_0 of the DLC film and induces transverse fracture of the film segments, as observed in the tensile experiments. Fracture can occur anywhere in the segments except within a distance l_c from the edges, where the tensile stress increases to the maximum from zero at the edge. For an overview of the theoretical models of the shear stress and tensile stress distribution in the film segments, one is referred to previous work [5,6]. Many transverse cracks form until the segments are divided into fracture patches such that the last patch to crack and the first patch to debond have approximately the same length l_d. The length distribution of the fracture patches at the final stage of straining is from $l_d/2$ to l_d. By measuring the length l_d of the fracture patches, the interfacial shear strength of a

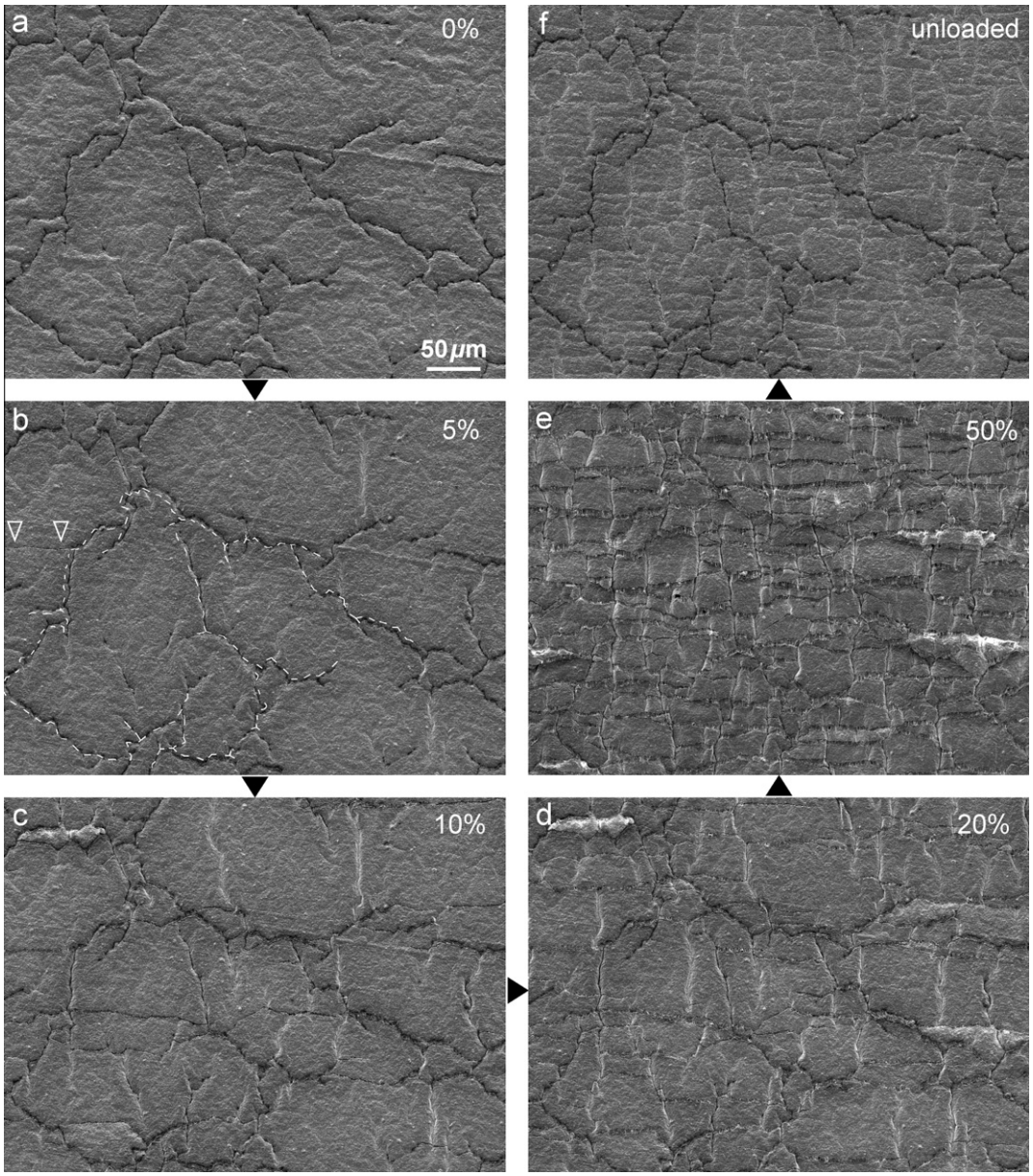

Fig. 5. Evolution of fracture patterns in DLC400–400 V film of large segments (188 μm) under stretching at the different strains indicated, with the loading direction along the vertical of the micrographs. The open arrows in (b) indicate the first transverse fracture crack and the dashed line marks the original form of the growth crack network before loading.

DLC film can be readily estimated according to the analytical model [5,6]:

$$\tau_0 = \frac{4t\sigma_0}{l_d} \tag{2}$$

where t is the thickness of the DLC film. For normal distribution of the patch lengths between $l_d/2$ and l_d, l_d can be approximated as $l_d = \frac{4}{3}\overline{L}$ [7], with $\overline{L}$ the average length of the fracture patches, which can be easily measured on SEM micrographs. Fig. 8 shows the length distribution of the fracture patches of DLC400–400 V and DLC 400–300 V films stretched to 50% strain, with average patch lengths $\overline{L}$ of 14 and 12.8 μm, respectively. Apparently, the spread of the patch lengths in both the strained films is much larger than 2-fold, with the ratio of the maximum length to the minimum length being about 6–7. This is mainly attributed to the growth defects of the DLC films induced by the rough surface of the rubber substrate and the filler particles exposed on the rubber surface. On the other hand, the minimum patch length of both films is 5 ± 0.5 μm, as measured at a high sampling frequency, and can be considered as $l_d/2$. Assuming $\sigma_0 = 1.67$ GPa for the DLC films [6], the interfacial shear strength of the two films with the same plasma treatment is estimated to be 108–200 MPa according to the measured $l_d = \frac{4}{3}\overline{L}$ and the minimum patch length ($l_d/2$). This shear strength is high and ensures strong adhesion of the DLC film segments to the HNBR substrate, with no debonding even under huge

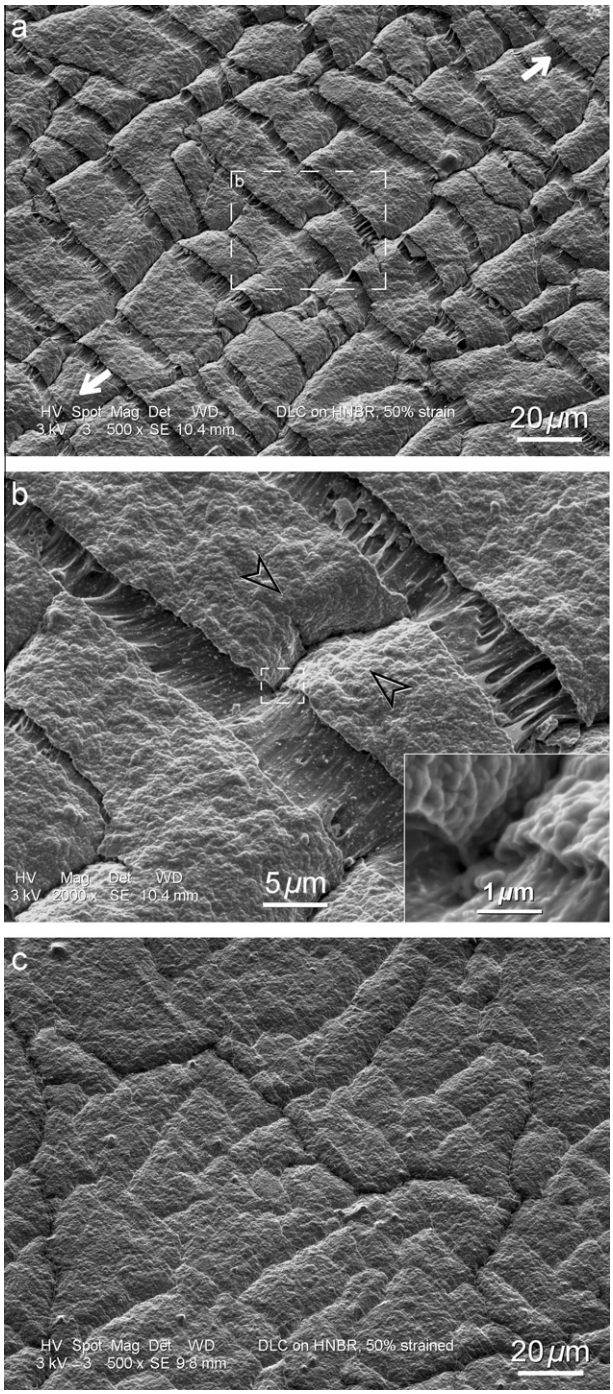

Fig. 6. SEM micrograph in a tilted view revealing the open transverse and close longitudinal fracture cracks in DLC400–400 V film segments under 50% strain with the strain direction indicated by two arrows (a), and viewed at higher magnification, with the inset of a close observation showing the well-bonded DLC film on HNBR cross the creased crack (b), with no delamination of the fractured DLC film segments observed after unloading (c).

deformation, as observed in the tensile tests. It is noteworthy that the DLC film of the finest segments has an average segment size (19 μm) close to those of fracture patches formed at 50% strain (12.8–14 μm). This means that the finest film segments are very flexible and hardly fracture under large deformation, e.g in a tribo-test wear track.

4. Discussion

The size of the film segments is related to the thermal mismatch strain, which depends on the ΔT exposed on the rubber substrate during deposition. The thermal mismatch strain between a DLC film and its rubber substrate arises due to the considerable difference in their coefficients of thermal expansion (CTE, α) and is usually described as:

$$\Delta\varepsilon = (\alpha_s - \alpha_f)\Delta T \tag{3}$$

where the subscripts f and s indicate the film and substrate, respectively. The crack spacing of a film having identical elastic properties as the substrate can be estimated as [8]:

$$l \cong \frac{5.6}{\varepsilon_0}\sqrt{\frac{\Gamma_f t_f}{\overline{E}}} \tag{4}$$

where Γ_f and t_f are the fracture energy and thickness of the film, and ε_0 is the applied strain or mismatch strain. For DLC film-coated rubber where the two materials have rather different elastic properties, the effective modulus $\overline{E}$ for equal biaxial stress condition needs to be modified to take into account the differences in properties and the thickness ratio between the DLC film and the rubber substrate [9]:

$$\overline{E} = \frac{E_s t_s}{E_s t_s + E_f t_f}\frac{E_f}{1-\nu_f} \tag{5}$$

where E is the modulus, ν is Poisson's ratio and t is the thickness of the DLC film or the rubber substrate.

Inserting Eqs. (3) and (5) into Eq. (4) yields [10]:

$$l \cong \frac{5.6}{(\alpha_s - \alpha_f)\Delta T}\sqrt{\frac{\Gamma_f t_f (1-\nu_f)(E_s t_s + E_f t_f)}{E_f E_s t_s}} \tag{6}$$

Consequently, the crack spacing is inversely proportional to ΔT, and also related to the fracture energy, effective modulus and thickness of the DLC film. To verify the validity of Eq. (6), $\Gamma_f = 35\ \mathrm{J\ m^{-2}}$ for DLC films [11,12] is used (other physical constants are listed in Table 1). We thus estimate the average crack spacing (equal to the average size of the film segments), and a good agreement between experiment and theory is attained, as seen in Fig. 3. The small deviation of the data points from the theoretical curve at large ΔT can be mainly attributed to the creep of polymer chains under high stress, so that the size of film segments observed is slightly larger than the predicted value.

It is anticipated that the cracks originate in the early stage of DLC film growth due to the thermal mismatch stress once a critical thickness is reached [8,13], then grow continuously with increasing film thickness. However, the cracking mechanisms of DLC films are different under tension and compression. With the thermal expansion of rubber substrate during a temperature rise (positive ΔT), which puts the growing DLC film under tension as schematically shown in Fig. 9a, the DLC film divides into microscaled segments at moment t_1 once it grows to the

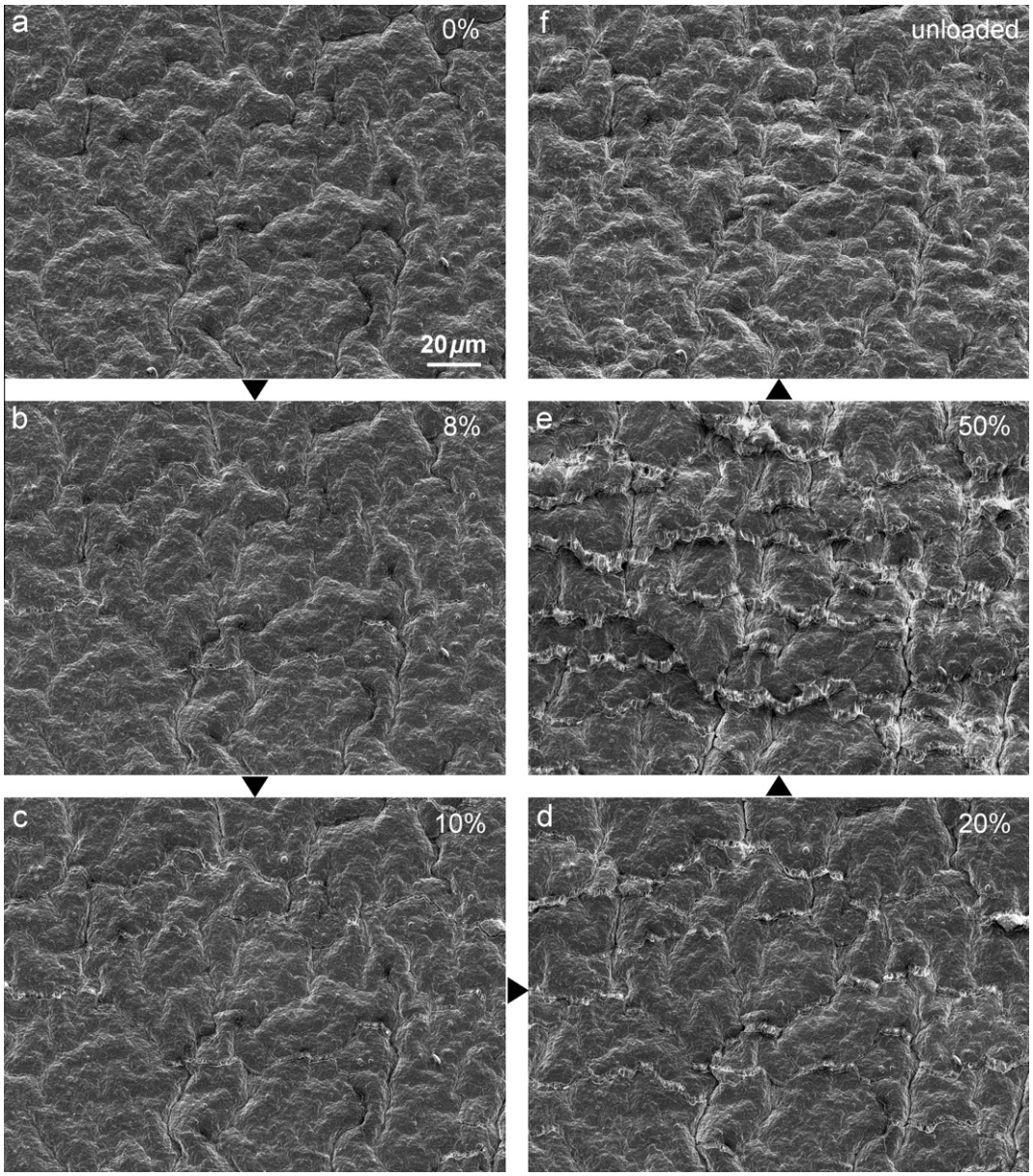

Fig. 7. Evolution of fracture patterns in DLC400–300 V film of fine segments (45 μm) under stretch of different strains indicated, with the loading direction along the vertical of the micrographs.

critical thickness at which the tensile stress reaches the ultimate strength of the DLC film. As the thermal expansion of the rubber substrate and deposition continue, the crack network surrounding the segments opens and the film segments grow both upwards and laterally. Since the rate of the temperature variation drops with deposition time as it approaches the equilibrium temperature but the deposition rate remains constant, the newly deposited DLC layer may bridge some of the cracks and combine a number of segments to form larger ones during the later stages of deposition, e.g. from moment t_3 to moment t_4. This means that the final size of the film segments is larger than the size of the initial ones. After the deposition is finished, the DLC film-coated rubber contracts during cooling from the equilibrium deposition temperature to room temperature. The film segments touch and push against each other, leading to the inward bending of the crack edges (see the last sketch at the finish t_f in Fig. 9a). The film segments themselves are relatively flat, and traces of the bridged cracks surrounding the initial smaller segments are visible, as shown in Figs. 2b and 4a. In contrast, the rubber substrate continuously contracts with decreasing temperature (negative ΔT) and brings the growing DLC film under compression, as shown in Fig. 9b. Once the compressive stress is high enough, the growing thin film becomes mechanically unstable and creases to form wrinkle cracks, which divide the film into segments at moment t_2. With continuous growth and compression, the film segments curve continuously. In the last phase of cooling to room temperature after the finish of deposition, the film segments curve further. It is notewor-

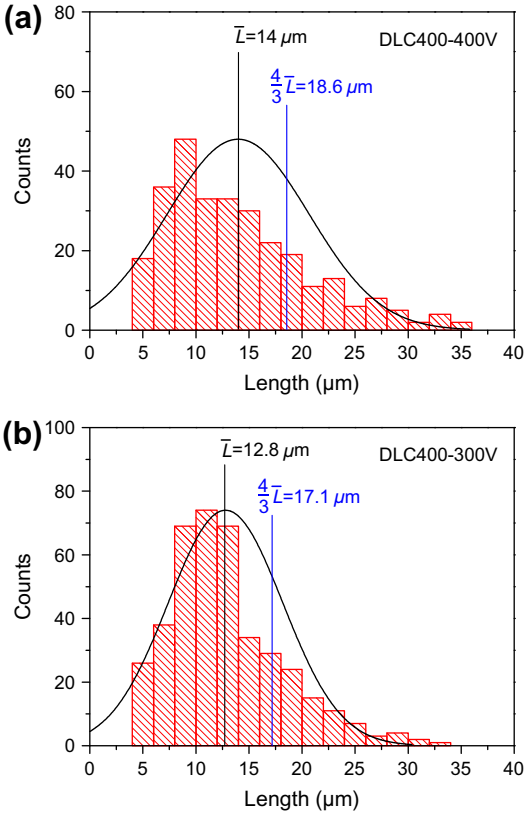

Fig. 8. Length distribution of fracture patches: (a) DLC400–400 V film and (b) DLC400–300 V film on HNBR substrate stretched to 50% strain.

Table 1
Modulus (E), thickness (t), CTE (α) and Poisson's ratio (v) of HNBR substrate and DLC film.

Properties	HNBR	DLC film
E (MPa)	10.2	150,000
t (μm)	2000	0.3
α ($\times 10^{-6}$ K^{-1})	180	6
v	0.5	0.13

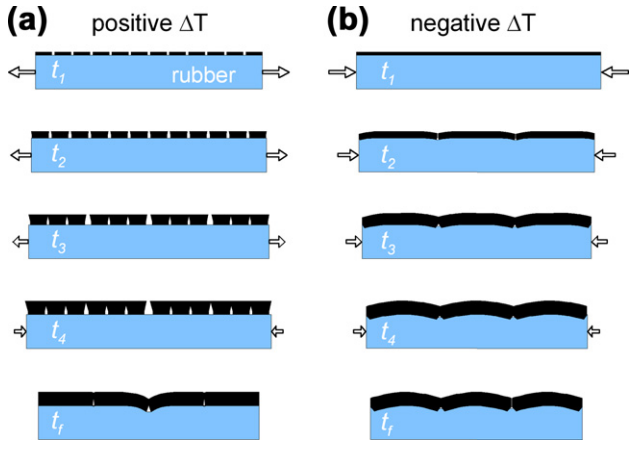

Fig. 9. Sketch of segmentation mechanism in different regimes of temperature variation during deposition: (a) positive ΔT and (b) negative ΔT. The length of the arrow pairs is indicative of the thermal expansion or contraction rate of the rubber substrate at different moments of deposition from t_1 to t_4. The cooling phase after deposition is from t_4 to t_f.

thy that the size of the segments does not increase from the initial one in this case, but, rather, becomes smaller if some of the segments fracture at their midpoint due to overbending. It is clear that the rate of temperature decrease in the early stage of deposition affects the final size of the film segments to a large extent. Based on this understanding of the different cracking mechanisms, a temperature change regime combining both positive and negative ΔTs together in a single deposition run could be used to control the size, curvature and edge bending extents of the film segments, as achieved in Fig. 2d.

The self-acting segmentation mechanisms are of importance for applications since the segment size of DLC films is on the micrometer scale and tunable. In this way we can control the density of the crack network or wrinkles without needing to use a net mask, as proposed in earlier work [1]. In particular, the cracks are closed and their edges bend inwards (see Fig. 4), which are crucial for preventing the formation of a large amount of wear debris that can cause wear and high friction in practical applications [2].

5. Conclusions

In summary, flexible DLC films of micrometer-scale segments have been deposited on HNBR rubber via self-acting segmentation. The size of the film segments can be tuned by controlling the temperature variation of the rubber substrate during deposition. The analytical description of crack spacing gives a good estimate of the segment size (equivalent to the crack spacing) and is a guide for the structural design of segmented DLC films for different applications. Clearly the dense crack network contributes to better flexibility and the ultralow friction of DLC film-coated HNBR rubber. The model and the experimental approach of film segmentation have also been applied to other kinds of rubber substrates, such as alkyl acrylate copolymer and nitrile butadiene rubbers, and the results confirm its validity [7]. It can be concluded that this work provides generic design rules for the deposition of flexible and low friction films on dynamic rubber seals and an approach to drastically reduce energy consumption in bearings and lubrication systems.

Acknowledgements

This research was carried out under the Project Number MC7.06247 in the framework of the research program of the Materials innovation institute (M2i), Delft, the Netherlands. Financial support from M2i is acknowledged.

References

[1] Aoki Y, Ohtake N. Tribol Int 2004;37:941.
[2] Pei YT, Bui XL, Zhou XB, De Hosson JTM. J Vac Sci Technol A 2008;26:1085.
[3] Bui XL, Pei YT, Mulder EDG, De Hosson JTM. Surf Coat Technol 2009;203:1964.

[4] Pei YT, Bui XL, Zhou XB, De Hosson JTM. Surf Coat Technol 2008;202:1869.
[5] Wheeler DR, Osaki H. In: Sacher E, Pireaux JJ, Kowalczyk SP, editors. ACS symposium series no. 440. Metallization of polymers. Washington (DC): American Chemical Society; 1990. p. 433.
[6] Ollivier B, Dowey SJ, Young SJ, Matthews A. J Adhes Sci Technol 1995;9:769.
[7] Schenkel M, Martinez-Martinez D, Pei YT, De Hosson JTM. Surf Coat Technol 2011;205:4838.
[8] Thouless MD, Olsson E, Gupta A. Acta Metall Mater 1992;40:1287.
[9] Kadolkar PB, Watkins TR, De Hosson JTM, Kooi BJ, Dahotre NB. Acta Mater 2007;55:1203.
[10] Pei YT, Bui XL, De Hosson JTM. Scripta Mater 2010;63:649–52.
[11] Wang JS, Sugimura Y, Evans AG, Tredway WK. Thin Solid Films 1998;325:163.
[12] Marques FC, Lacerda RG, Champi A. Appl Phys Lett 2003;83:3099.
[13] Atkinson A, Guppy RM. J Mater Sci 1991;26:3869.